First principles dynamic modeling and multivariable control of a cryogenic distillation process

Betlem, B.H.L.; Roffel, B.; de Ruijter, J.A.F.

Published in:
Computers %26 Chemical Engineering

DOI:
10.1016/S0098-1354(00)00313-6

Publication date:
2000

ELSEVIER

Computers and Chemical Engineering 24 (2000) 111–123

Computers & Chemical Engineering

www.elsevier.com/locate/compchemeng

First principles dynamic modeling and multivariable control of a cryogenic distillation process

B. Roffel [a,*], B.H.L. Betlem [a], J.A.F. de Ruijter [b]

[a] *University of Twente, Faculty of Chemical Engineering, PO Box 217, 7500 AE Enschede, The Netherlands*
[b] *KEMA Netherlands bv, PO Box 9035, 6800 ET Arnhem, The Netherlands*

Received 10 August 1998; received in revised form 1 March 2000; accepted 1 March 2000

Abstract

In order to investigate the feasibility of constrained multivariable control of a heat-integrated cryogenic distillation process, a rigorous first principles dynamic model was developed and tested against a limited number of experiments. It was found that the process variables showed a large amount of interaction, which is responsible for the difficulties with the presently used, PID-based, control scheme, especially in load-following situations, which are common in air separation plants such as for instance integrated coal gasification combined cycle plants. Contrary to what is suggested in the literature, it was found that vapor hold-up in low-temperature, high-pressure columns does not play a significant role in the process dynamics. Despite large throughput changes and non-linear process behavior, multivariable model predictive control using a linearized model for average operating conditions, could work well provided all process flows have sufficient range. Due to the strong interactive nature of the process variables, process changes have to be made slowly, since otherwise manipulated variables easily saturate and process output targets cannot be maintained.

Keywords: Dynamic modeling; Multivariable control; Cryogenic distillation

1. Introduction

Distillation is used in the chemical industry for the separation of a mixture of components. Heat is supplied at the bottom of the column in order to evaporate the mixture and heat is withdrawn at the top of the column in order to condense the volatile components. The dynamics and control of ordinary distillation towers has been studied extensively (Skogestad, 1992).

Cryogenic distillation is similar to ordinary distillation, however, the process takes place at extremely low temperatures. This is necessary if one wants to separate air for example, in its basic components oxygen and nitrogen (Mandler, Vinson & Chatterjee, 1989). Only at low temperatures (around 100 K) will these components become liquid and can they be separated in the column.

In an air distillation column, nitrogen is the most volatile component and will therefore be present in high concentration in the top of the column. If one wants to condense nitrogen, a cooling medium would be required with a lower boiling point than nitrogen. This poses a problem since a very costly installation would be required to achieve these low temperatures in the condenser.

An ideal solution is to integrate the reboiler and the condenser; energy, which is withdrawn in the condenser is used in the reboiler. To achieve this, the distillation column is split into two smaller columns, one operating at a low pressure hence the boiling point of the mixture will also be low. The second column operates at a higher pressure resulting in a higher boiling point of the mixture. The difference in boiling points due to the difference in pressure becomes the driving force for the transfer of energy in the integrated reboiler–condenser. A typical layout is shown in Fig. 1. The lower part of the column is the high-pressure column and the upper part the low-pressure column. The integrated reboiler–condenser is usually located in the bottom of the low-

* Corresponding author.
E-mail addresses: dcp@ct.utwente.nl (B. Roffel), dcp@ct.utwente.nl (B.H.L. Betlem), j.a.f.deruijter@kema.nl (J.A.F. de Ruijter)

0098-1354/00/$ - see front matter
PII: S0098-1354(00)00313-6

pressure column. Air is fed to both columns but mainly to the high-pressure column, the main feed to the low-pressure column is a crude oxygen flow, the pressure of the low-pressure column is controlled at a feed dependent target. The pressure of the high-pressure column is mainly determined by the feed flow. If the feed flow to the HP column changes, the heat transfer in the reboiler–condenser changes, thereby effecting the pressure. A typical distillation column contains in the order of 40–80 trays.

Because of the heat integration, the process variables show a large amount of interaction and multivariable control is deemed necessary to achieve good purity control of the various outlet flows.

Gross, Baumann, Geser, Rippin and Lang (1998) recently made a controllability analysis of a heat-integrated process by rigorous modeling, model identification and analysis. The authors, however, only studied product quality control structures (4×4 system), whereas in our case three concentrations and two levels have to be controlled. In addition, our industrial columns do not have an auxiliary reboiler and/or condenser, which create additional degrees of freedom. In our situation most of the vapor coming from the top of the high pressure column is condensed and used for evaporation of liquid in the low pressure column, thereby creating a large amount of interaction between the two columns.

2. Model description

The model for distillation columns generally consists of differential equations for the mass and energy balances around each tray and a set of algebraic equations consisting of equations for the tray pressure drop,

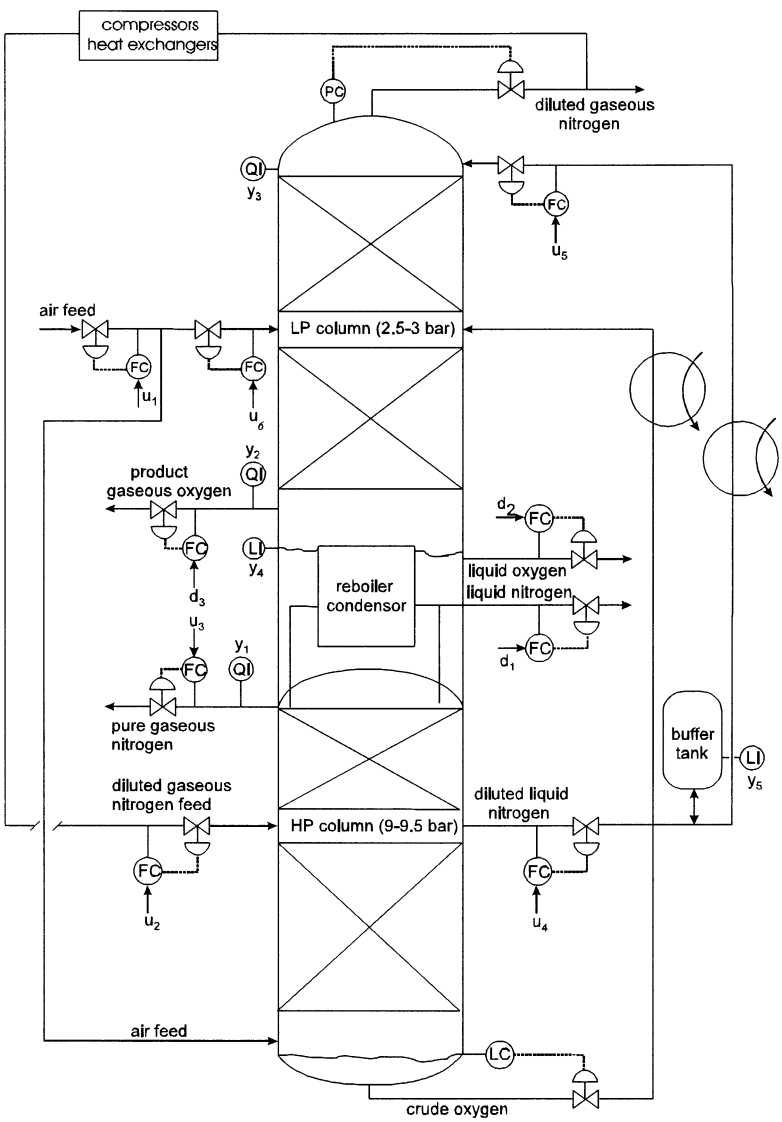

Fig. 1. Schematic diagram of a cryogenic distillation process.

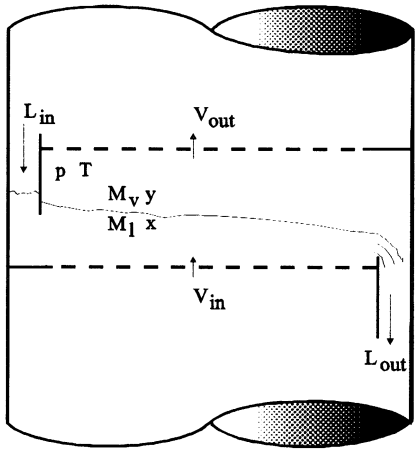

Fig. 2. Schematic of a tray and nomenclature.

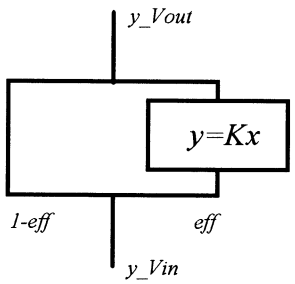

Fig. 3. Effect of tray efficiency on concentration.

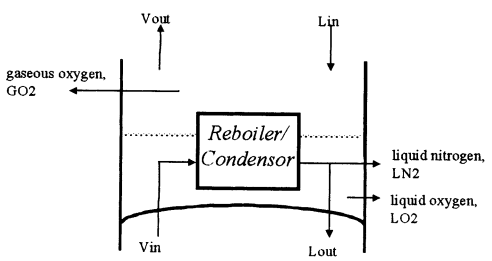

Fig. 4. Schematic overview of the reboiler–condenser.

liquid flow from the tray, liquid aeration, phase equilibrium, physical properties and a number of boundary conditions. A detailed mathematical model of a tray would become extremely complex if no assumptions or a-priori simplifications would be made.

In this study they are:

- the liquid and vapor are ideally mixed, hence there are no concentration gradients on a tray;
- the liquid and vapor which are in contact are in thermal equilibrium;
- the pressure and temperature on a tray are uniform
- weeping and entrainment can be ignored (follows from static design calculations);
- the tray efficiency is constant and does not depend on column loading.

For the symbols that are used in the model description, one is referred to the nomenclature and Fig. 2.

The base model for the columns is given in Appendix A, the model consists of the common mass and energy balances and additional equations. In this section the additions and simplifications to the base model will be discussed.

3. Integrated reboiler–condenser

The top vapor flow of the high-pressure column condenses in the condenser and generates the vapor flow for the low-pressure column (see Fig. 4).

In modeling the reboiler–condenser, the following assumptions were made:

- the vapor flow to the condenser will be totally condensed and all liberated heat will used in the reboiler;
- the reboiler behaves like a normal tray, the additional term is the added energy from the condenser. The same assumptions therefore apply as were made for a tray, such as vapor-liquid equilibrium and so forth.

The energy that is being transferred can be calculated from:

$$Q = UA\ (T_{\mathrm{V,top}} - T_{\mathrm{L,bottom}}) \tag{1}$$

This energy is extracted from the condensing vapor, hence:

$$Q = F_{\mathrm{Vin}}(h_{\mathrm{Vin}} - h_{\mathrm{Lout}}) \tag{2}$$

The mass balance for the condenser is:

$$F_{\mathrm{Vin}} = F_{\mathrm{Lout}} + F_{\mathrm{LN2}} \tag{3}$$

and the component balance becomes:

$$y_{\mathrm{Vin,c}} = x_{\mathrm{Lout,c}} = x_{\mathrm{LN2,c}} \quad \forall\, c \in \{1\,..\,\mathrm{nocomp}\} \tag{4}$$

The total mass and mass balance for component c at the reboiler side can be given by:

$$Mc_{\mathrm{c}} = M_{\mathrm{v}} y_{\mathrm{Vout,c}} + M_{\mathrm{l}} x_{\mathrm{LO2,c}} \quad \forall c \in \{1\,..\,\mathrm{nocomp}\} \tag{5}$$

$$\frac{\mathrm{d}Mc_{\mathrm{c}}}{\mathrm{d}t} = F_{\mathrm{Lin}} x_{\mathrm{Lin,c}} - F_{\mathrm{Vout}} y_{\mathrm{Vout,c}} - F_{\mathrm{LO2}} x_{\mathrm{LO2,c}} - F_{\mathrm{GO2}} y_{\mathrm{Vout,c}} \quad \forall\, c \in \{1\,..\,\mathrm{nocomp}\} \tag{6}$$

The total mass is calculated from the sum of the mass of the individual components. The energy content is defined by:

$$E = M_{\mathrm{V}} h_{\mathrm{Vout}} + M_{\mathrm{l}} h_{\mathrm{LO2}} + M_{\mathrm{t}} c_{\mathrm{t}} (T_{\mathrm{LO2}} - T_{\mathrm{ref}}) \tag{7}$$

and the energy balance by:

$$\frac{\mathrm{d}E}{\mathrm{d}t} = F_{\mathrm{Lin}} h_{\mathrm{Lin}} - F_{\mathrm{Vout}} h_{\mathrm{Vout}} - F_{\mathrm{LO2}} h_{\mathrm{LO2}} - F_{\mathrm{GO2}} h_{\mathrm{GO2}} + Q \tag{8}$$

The overall heat transfer coefficient was determined experimentally from operating data and it was found to be dependent on the vapor flow to the condenser:

$$UA = c_1 F_{\mathrm{Vin}}^{0.8} \tag{9}$$

The vapor-liquid equilibrium equation is similar to Eq. (A13); the physical property equations are similar to Eqs. (A15)–(A21) and the miscellaneous equations similar to the equations for a tray.

4. Vapor flow/pressure dynamics

The energy balance for a tray is equivalent to a pressure balance, under the assumption that concentration changes are slow compared to pressure changes, which is shown by Rademaker, Rijnsdorp and Maarleveld (1975).

The mass and energy balance can be combined and written as:

$$(C_{p,\rho} + C_{p,T}) \frac{\mathrm{d}p}{\mathrm{d}t} = F_{\mathrm{Vin}} - F_{\mathrm{Vout}} \tag{10}$$

with:

$$C_{p,\rho} = \bar{V} \left(\frac{\partial \rho}{\partial p} \right)_y \tag{11}$$

$$C_{p,T} = \frac{(M_{\mathrm{v}} c_{\mathrm{v}} + M_{\mathrm{l}} c_{\mathrm{l}} + M_{\mathrm{t}} c_{\mathrm{t}})}{\Delta H_{\mathrm{c}}} \left(\frac{\partial T}{\partial p} \right)_x \tag{12}$$

For the high-pressure column under investigation, including the condenser, it can be calculated that the column capacity due to compressibility effects $C_{p,\rho} = 0.33$ kmol bar^{-1} and the column capacity due to thermal effects $C_{p,T} = 0.24$ kmol bar^{-1}, hence the total capacity is 0.57 kmol bar^{-1}.

The resistance for flow changes, $\partial(\Delta p)/\partial F_{\mathrm{V}}$, can be calculated from the equation for the dry tray pressure drop. For average conditions in the high-pressure tower we may write: $\Delta p_{\mathrm{dry}} = 0.0002 F_{\mathrm{Vin}}^2$, from which the resistance R becomes 0.0008 bar s kmol^{-1}. The time constant for pressure or flow changes therefore becomes $t = RC = 0.0008 \times 0.57 = 0.0005$ s.

Hence the flow and pressure changes are extremely fast and can be considered momentary. The enthalpy balance could therefore be simplified to a static enthalpy balance and the capacities for flow and pressure changes could be lumped, such that Eq. (10) is written for the entire column, including the combined reboiler–condenser.

In this case the energy balance for a tray could be simplified to:

$$F_{\mathrm{Vin}} h_{\mathrm{Vin}} + F_{\mathrm{Lin}} h_{\mathrm{Lin}} - F_{\mathrm{Vout}} h_{\mathrm{Vout}} - F_{\mathrm{Lout}} h_{\mathrm{Lout}} = 0 \tag{13}$$

Subtracting the total mass balance will then result in:

$$F_{\mathrm{Vout}} = F_{\mathrm{Vin}} \frac{h_{\mathrm{Vin}} - h_{\mathrm{Lout}}}{h_{\mathrm{Vout}} - h_{\mathrm{Lout}}} + F_{\mathrm{Lin}} \frac{h_{\mathrm{Lin}} - h_{\mathrm{Lout}}}{h_{\mathrm{Vout}} - h_{\mathrm{Lout}}} \tag{14}$$

The second term in the right hand side of Eq. (14) is usually small ($\sim 0.2\%$ of the first term in this case), hence it could be ignored and the enthalpy balance could be simplified to:

$$F_{\mathrm{Vout}} = F_{\mathrm{Vin}} \frac{h_{\mathrm{Vin}} - h_{\mathrm{Lout}}}{h_{\mathrm{Vout}} - h_{\mathrm{Lout}}} \tag{15}$$

Section 5 will show the impact of a number of simplifications on the dynamic behavior.

5. Simulations

First a number of simulations were carried out to determine the impact of the vapor hold-up on the dynamics.

In case the vapor hold-up is negligible, Eq. (A1) can be simplified to:

$$M c_{\mathrm{c}} = M_{\mathrm{l}} x_{\mathrm{Lout,c}} \tag{16}$$

and Eq. (A4) can be written as:

$$E = M_{\mathrm{l}} h_{\mathrm{Lout}} + M_{\mathrm{t}} c_{\mathrm{t}} (T_{\mathrm{Lout}} - T_{\mathrm{ref}}) \tag{17}$$

while Eq. (A22) can be omitted. The last two equations are useful, since they can be substituted into Eqs. (A2) and (A5), respectively and the new Eqs. (A2) and (A5) are easier to solve then their original counterpart.

It was found that ignoring the vapor holdup showed hardly any impact on the concentration responses. Fig. 5 shows the response of the oxygen concentration in the pure nitrogen flow from the high-pressure column as a response to a negative step change in the feed flow to the high-pressure column. The dotted line gives the response of the model without vapor hold-up, the solid line the model response with vapor hold-up, the points indicate measurements from the industrial column. As can be seen, there is no major impact on the composition response when the vapor hold-up is ignored. The only model parameters which were used to fit the experiments to the model predictions were coefficient c_1 in Eq. (9) and the tray efficiency (Eq. (A14)).

Fig. 6 shows the response of the nitrogen concentration (impurity) in the LP column gaseous oxygen flow to a step change HP column feed flow, Fig. 7 shows the

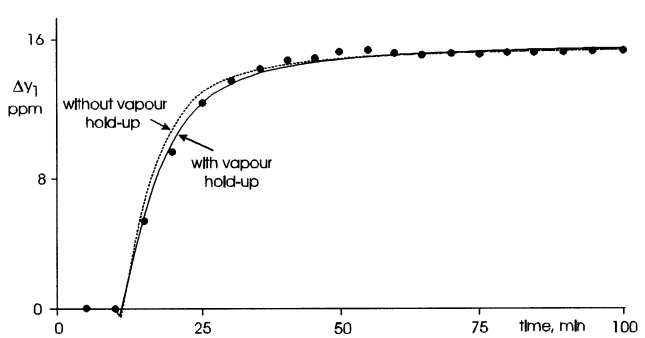

Fig. 5. Response of the change in oxygen concentration (ppm) in pure nitrogen flow from HP column to a step change in HP feed.

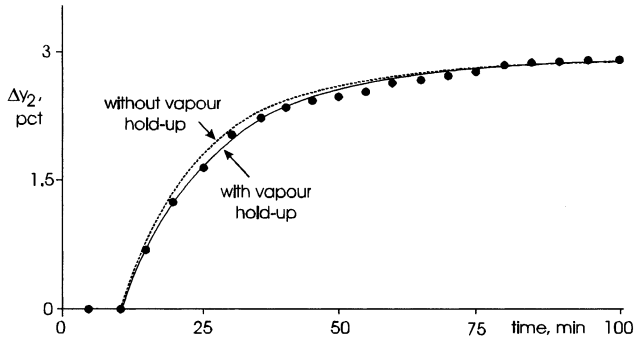

Fig. 6. Response of the change in oxygen concentration (pct) in oxygen flow from LP column to a step change in HP feed.

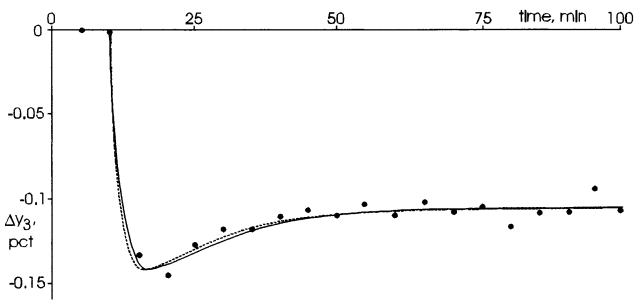

Fig. 7. Response of the change in oxygen concentration (pct) in dilute nitrogen flow from LP column to a step change in HP feed.

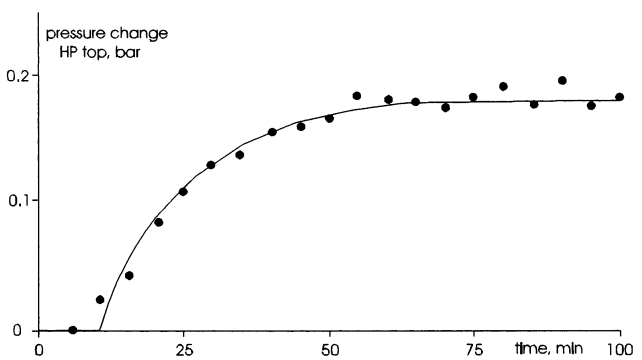

Fig. 8. HP column top pressure response to change in HP column feed.

response of the oxygen concentration in the LP column dilute nitrogen flow to a step change in HP column feed flow.

All responses show a minor influence of the vapor hold-up, in all cases the response without vapor hold-up is slightly faster. This is in contradiction with the literature (Luyben, 1992), where it is suggested to include vapor hold-up in the model for high pressure, low temperature columns. As was shown this strongly depends on the capacity for pressure changes and the resistance to flow changes.

Fig. 8 shows the response of the pressure change in the top of the high-pressure column upon a step change in the high pressure column feed flow. As can be seen, the model predictions and the measurements are in rather good agreement.

6. Control study

Since the present control configuration using PID controllers, gain scheduling and feed-forward control does not function very well in load-following applications, a control study was undertaken to determine whether the tower system can be controlled by a multivariable controller. The following variables were defined for the control study (see also Fig. 1):

y_1 = ppm oxygen in pure gaseous nitrogen flow from HP column;
y_2 = pct nitrogen in gaseous oxygen flow from LP column;
y_3 = pct oxygen in dilute nitrogen flow from LP column;
y_4 = bottom level LP column;
y_5 = bottom level reflux drum;

u_1 = total air flow;
u_2 = diluted gaseous nitrogen flow to HP column (reflux);
u_3 = pure gaseous nitrogen flow from HP column;
u_4 = diluted liquid nitrogen flow from side of HP column;
u_5 = diluted liquid nitrogen flow to top of LP column (reflux);
u_6 = air flow to LP column;

d_1 = liquid nitrogen flow from top of HP column (demand);
d_2 = liquid oxygen flow from bottom of LP column (constant demand);
d_3 = gaseous oxygen flow from bottom of LP column (constant demand),

in which y = controlled variable, u = manipulated variable and d = disturbance variable.

The level in the bottom of the HP column was not included in this study, since its conventional control did not pose any problems.At normal operating conditions (NOC, Table 1), the column operates at approximately 85% of its maximum load.

In addition to the constraints shown in Table 1, the following constraints are active for the manipulated variables:

$0.0 \le u_1 \le 1.6\ u_{1,\mathrm{NOC}}$;
$0.0 \le u_2 \le 2.0\ u_{2,\mathrm{NOC}}$;
$0.0 \le u_3 \le 2.0\ u_{3,\mathrm{NOC}}$;
$0.0 \le u_4 \le 1.5\ u_{4,\mathrm{NOC}}$;
$0.0 \le u_5 \le 1.5\ u_{5,\mathrm{NOC}}$;
$0.5u_{6,\mathrm{NOC}} \le u_6 \le 2.0u_{6,\mathrm{NOC}}$;

The flow of oxygen to the next part of the process should have a minimum purity of oxygen, the level in

Table 1
Normal operating conditions (NOC) based on an arbitrary feed rate of 100 kmol min^{-1}

Process inputs (kmol min^{-1})	Process outputs	Disturbances (kmol min^{-1})	Constraints
$u_1 = 100.00$	$y_1 = 56.74$ ppm O_2	$d_1 = 0.066$	
$u_2 = 1.81$	$y_2 = 6.95\%$ N_2	$d_2 = 0.069$	$y_2 \leq 8.0\%$ N_2
$u_3 = 10.24$	$y_3 = 1.61\%$ O_2	$d_3 = 21.41$	
$u_4 = 34.63$	$y_4 = 52.01\%$		$40 \leq y_4 \leq 60\%$
$u_5 = 34.63$	$y_5 = 50.00\%$		$10 \leq y_5 \leq 90\%$
$u_6 = 4.36$			

the reflux drum should stay between 10 and 90%, the level in the low pressure column has to stay within narrower limits in order to avoid that the reboiler–condenser is not sufficiently covered by liquid and heat transfer area is subsequently lost.

The manipulated variables all have lower and upper limits dictated by the size of the valve, the lower limit for the flow to the low pressure column, however, should not become zero, it was assumed that a lower value of 50% of the flow at normal operating conditions should be maintained.

Since the confidence in the first principles model is good, step weight models were derived from the detailed model at minimum and maximum column load. Table 2 gives an indication of the ratio in values of the manipulated variables and disturbance variables at minimum and maximum load.

As can be seen, the flow through the columns varies significantly and it may be expected that the dynamics of the transfer functions between manipulated and controlled variables will also vary significantly. In addition, column behavior is expected to be non-linear. Fig. 9 shows the transfer functions at minimum column load, Fig. 10 the transfer functions at maximum load. The models show 30 stepweights, with a sampling interval of 4 min. This value was selected on the basis of a rule of thumb, which states that an effective controller execution interval should be less than or equal to one third of the major time constant of the process model. As can be seen from Figs. 9 and 10 a value of 4 min should be adequate for y_1 and y_2 and certainly for control of level in this case, the value may be somewhat high for control of y_3, however, for reasons of implementation a value of 4 min is preferred.It can be seen that most of the gains in the process models change considerably, in some cases also the dynamics have changed considerably, for example for (y_3,u_3).

As can be seen from Fig. 10, both levels y_4 and y_5 can only be effectively controlled by using manipulated variables u_4 and u_5. When we do not consider the effect of the manipulation of u_4 and u_5 on y_1 to y_3, we are left with a system with three output variables and four input variables.

If one of the input variables is selected as degree of freedom for optimization, the Relative Gain Array values for the remaining square system can be computed. The results for maximum load are shown in Table 3. As can be seen from this simple analysis, tower feeds u_1 or u_2 are primary candidates to be used as degree of freedom for optimization, since the remaining pairing of input-output variables is most attractive in these cases. There is still some interaction from other control loop pairings and both level control loops will also affect control performance in a negative way. If u_2 was chosen as degree of freedom, the following structure would result: (y_2,u_1), (y_1,u_3) and (y_3,u_6).

However, u_4 and u_5 affect y_2 more than u_1 does, a similar situation exists for the pair (y_3,u_6). Hence, the single loop control concept is not very attractive for this reason and multivariable control will be studied as an alternative.

It is preferred that the multivariable controller with fixed settings controls the process at minimum and maximum process conditions rather than using an adaptive multivariable controller. Therefore controller design and performance was tested at two extremes: using a process model at minimum load (denoted by Pmin) and a controller design at maximum load (denoted by Cmax) and vice versa.

Introducing set-point changes in y_1 and y_5, Fig. 11 shows the changes in process outputs (in percent of the original starting value) for the combinations (Cmax, Pmax) and (Cmax, Pmin); the controller design parameters are given in Table 4. For all multivariable controller plots (Figs. 11–16) the time is expressed as a multiple of the controller execution interval.

Fig. 12 shows the changes in process inputs (also in

Table 2
Ratio between variables at maximum and minimum flows

Manipulated variable	Ratio	Disturbance variable	Ratio
u_1	1.9	d_1	1.0
u_2	1.2	d_2	1.0
u_3	1.2	d_3	1.9
u_4	2.2		
u_5	2.2		
u_6	1.1		

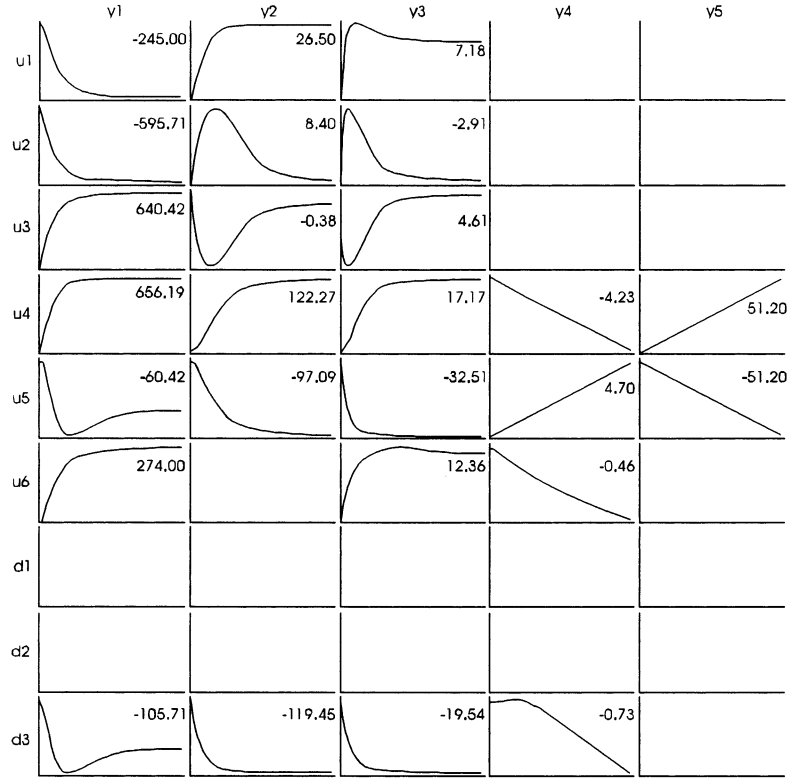

Fig. 9. Process models at minimum load.

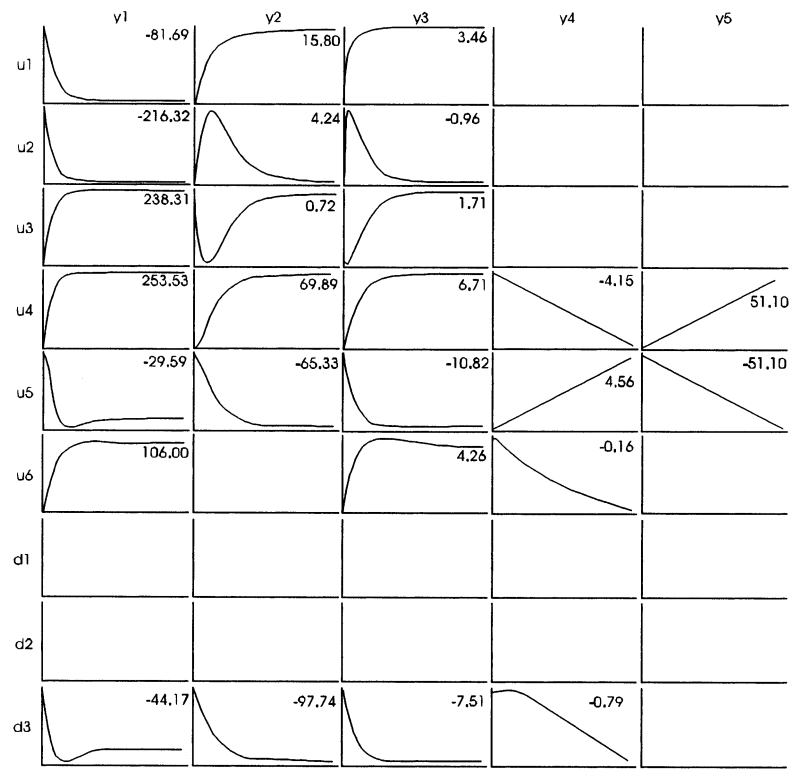

Fig. 10. Process models at maximum load.

percent of original starting value) for the same combinations. It was found that the change in total feed u_1 is small, the value of u_6 (air feed to low pressure column) shows a large change in relative terms. This flow is normally very small, hence the feed to the high-pressure tower does not change significantly.

Table 3
RGA values for different input-output combinations

u_1 degree of freedom				u_2 degree of freedom			
	y_1	y_2	y_3		y_1	y_2	y_3
u_2	0.16	0.86	−0.02	u_1	0.02	0.96	0.02
u_3	1.04	0.14	−0.18	u_3	1.17	0.04	−0.21
u_6	−0.20	0.00	1.20	u_6	−0.19	0.00	1.19
u_3 degree of freedom				u_6 degree of freedom			
u_1	−0.15	1.31	−0.16	u_1	0.26	−0.91	1.65
u_2	1.47	−0.31	−0.16	u_2	−2.16	1.67	1.49
u_6	−0.32	0.00	1.32	u_3	2.90	0.24	−2.14

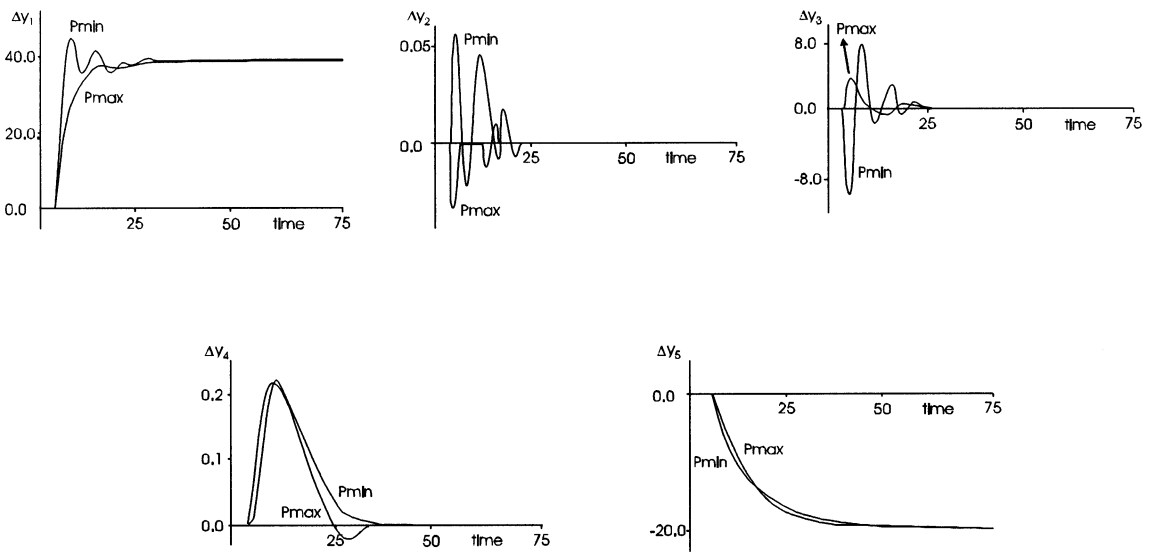

Fig. 11. Process output responses to a step change in y_1 and y_5 set-point using controller design at maximum process conditions with the process at minimum and maximum conditions respectively.

It can also be seen from Figs. 11 and 12 that when the controller is designed for maximum process conditions (Cmax) and the process is also at maximum conditions (Pmax), control is very stable. When the controller is designed based on the model at maximum load but the process is at minimum load (Pmin), the process responses show some slight oscillations, although control behavior is still acceptable. Apparently, both levels (y_4 and y_5) are far less sensitive to modeling errors than their non-integrating counterparts (y_1 to y_3). Acceptable control performance is achieved by using rather large weights on the process inputs (see Table 4); this serves the purpose of avoiding controller input saturation and suppressing process/model mismatch. When the input weights are low, the process responses are not always stable when the process model changes and one or more of the process inputs easily saturates at its maximum or minimum constraint. In the latter case it takes up to 150 sampling intervals before the process responses dampen out. It was therefore concluded that due to the selection of high inputs weights, one multivariable controller with fixed settings can be used for the entire operating region of the process. Set-point changes are reached in an acceptable time, which is still much smaller than the open loop response time.

As set-point changes are not occurring very often, it will be good to also test the controller behavior for changes in measurable disturbances. The flow of gaseous oxygen (d_3) is the most common disturbance. Control system performance was checked for a step disturbance in d_3 of + 10%. Fig. 13 shows the deviation

Table 4
Controller design parameters

Manipulated variable	
Control horizon	[3, 3, 3, 3, 3, 3]
Weighting parameter	[10,50,50,100,50,200]
Output variable	
Prediction horizon	[24, 24, 24, 24, 24]
Weighting parameter	[0.0001, 1.0, 0.25, 0.25, 0.0001]

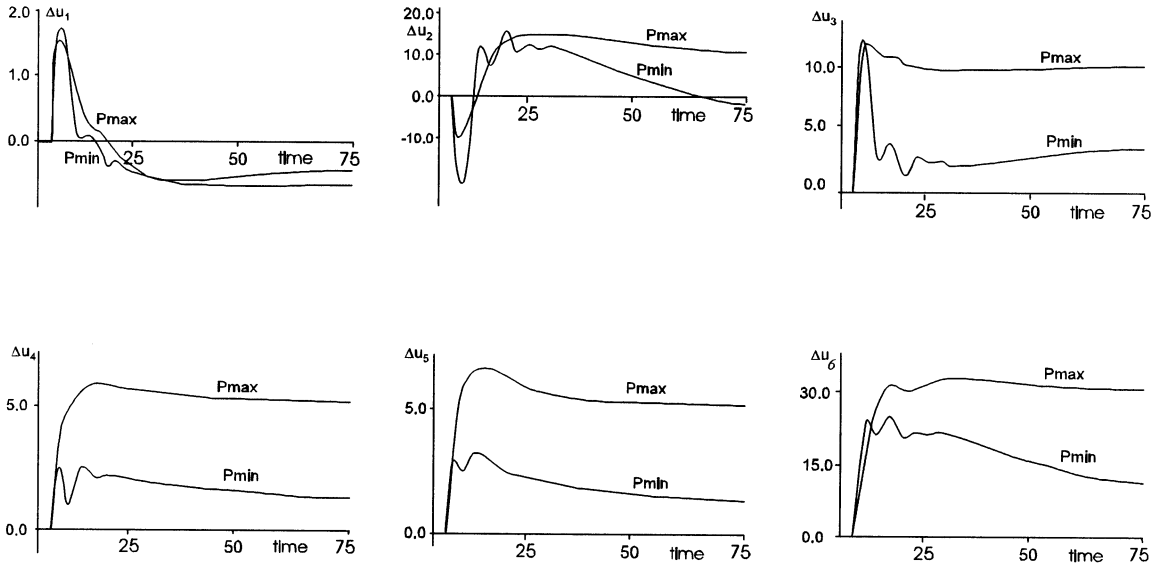

Fig. 12. Process input responses to a step change in y_1 and y_5 set-point using controller design at maximum process conditions with the process at minimum and maximum conditions respectively.

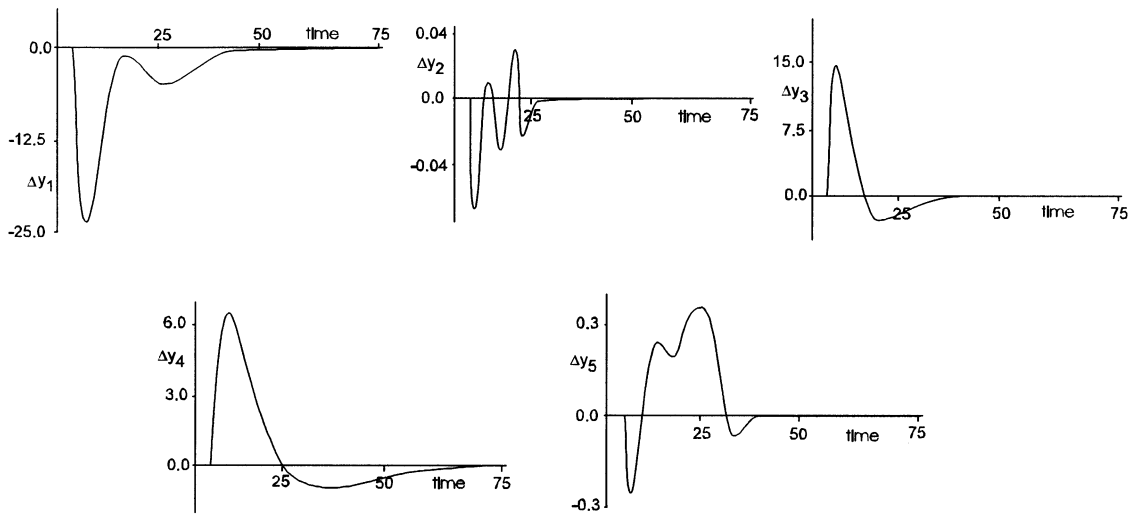

Fig. 13. Response of process outputs to a step disturbance in d_3, using multivariable control.

in process outputs y_1 to y_5 (in percent of their original starting values). It can be seen that y_1 is affected temporarily by as much as 25%, y_3 up to 15% and y_4 up to 6%, whereas y_2 and y_5 are hardly affected by this step disturbance. Note that y_2 is the oxygen concentration of the flow of oxygen which is used in the next process!

Fig. 14 shows the process-input changes for this case. As can be seen, u_2 changes by approximately a factor of 2 (100%), which is also the constraint value. Intuitively this can be explained by looking at Fig. 1. The flow d_3 is the vapor draw-off from the bottom of the low-pressure tower, it can only be increased by vaporizing more liquid, which can be achieved, amongst others, by increasing the flow to the high-pressure column u_2. When larger disturbances are given in d_3, u_2 will remain at its constraint value and other process inputs are adjusted to eliminate the disturbance, which is a much slower process. Disturbance rejection properties of the multivariable controller are found to be very acceptable.The responses of the process variables using the conventional control scheme are shown in Figs. 15 and 16. The average values of the tuning parameters as well as the control loop pairings for the industrial column are given in Table 5.

This control loop selection may not be a very logical choice, as the analysis in Table 3 shows. However, despite possibilities for better pairings, interaction would remain when another single loop control concept would be applied to the columns.

Of the control scheme as implemented by the manufacturer, the first controller uses gain scheduling where the gain depends on the operating conditions, the third controller used gain and integral time scheduling, depending on the operating conditions; to the output of the fourth controller a bias term was added, which depended on the LP column mass balance.

As can be seen, flow u_3 is not used in the conventional control scheme to control a process output. The set-point of flow controller u_3 was set depending on the air flow to the HP column and the airflow to the LP column. The latter control can be seen as a feed-forward controller.

Control of y_2 is superior in the multivariable case (maximum deviation -0.055 versus -48.3%). In addition, control of y_4 (LP bottom level) shows a slow decrease using the conventional control scheme, this decrease continues for longer times and eventually the level reaches its minimum constraint. As can be seen from Fig. 16, u_6 (LP column feed) is held at its original value. This is due to the fact that the change in control signal from the feedback controller (due to decreasing LP column level) is eliminated by the change in bias signal.

A thorough redesign of the conventional control scheme would be required to achieve better control.

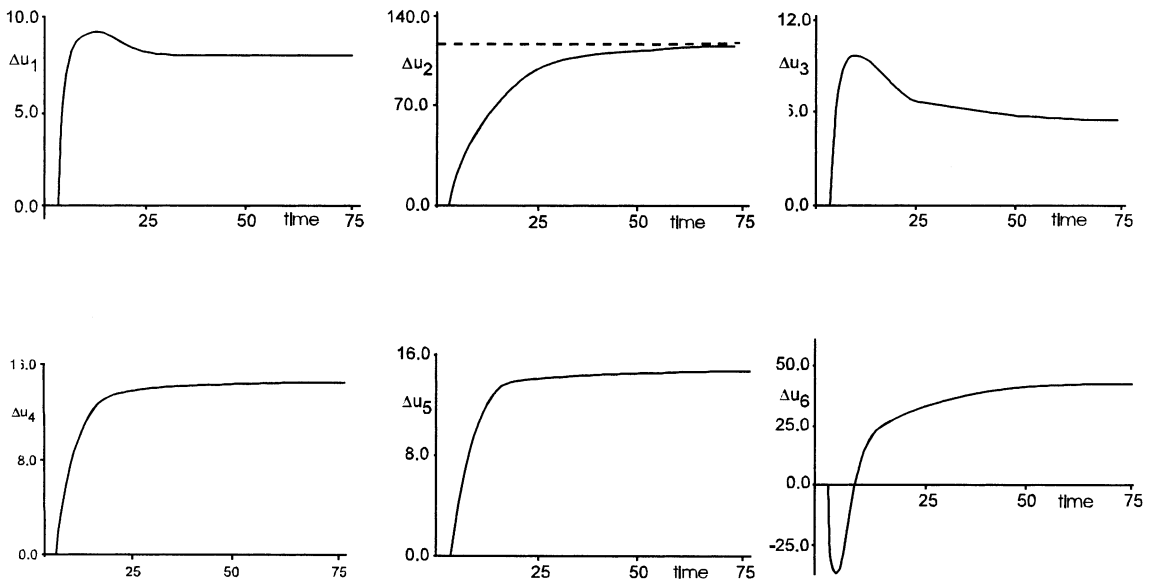

Fig. 14. Responses of process inputs to a step disturbance in d_3, using multivariable control.

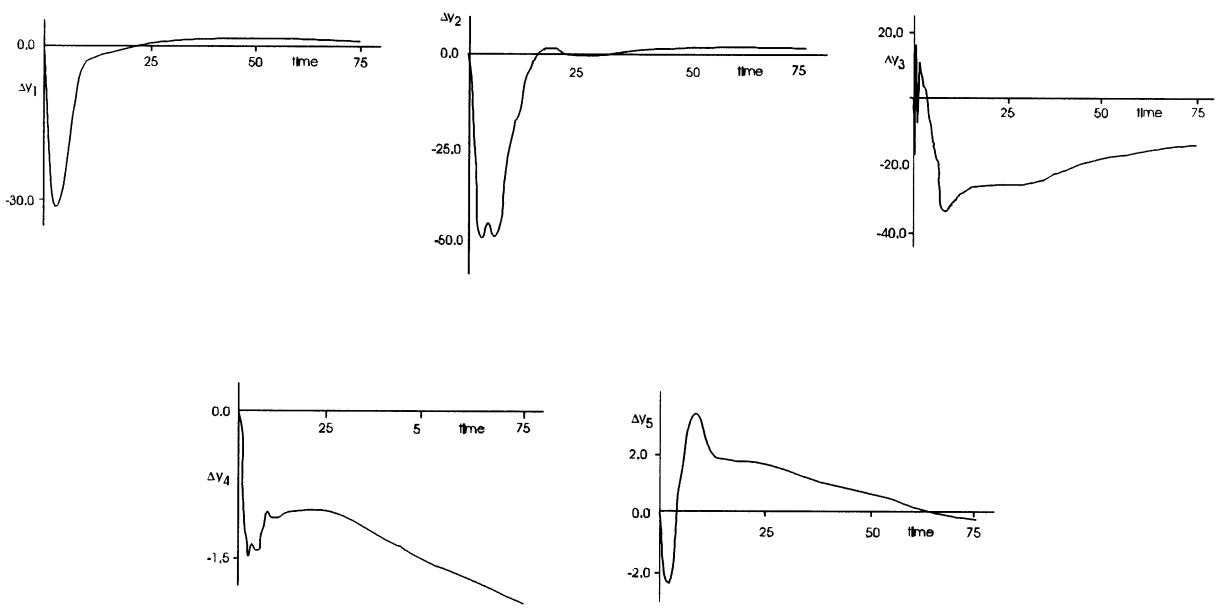

Fig. 15. Response of process outputs to a step disturbance in d_3, using conventional control.

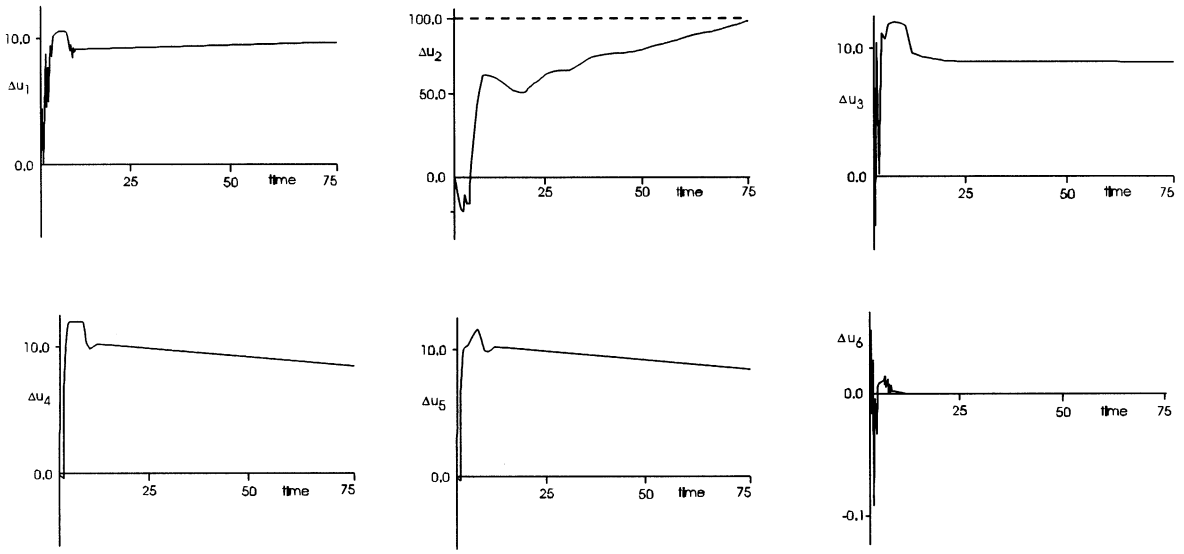

Fig. 16. Responses of process inputs to a step disturbance in d_3, using conventional control.

Table 5
Conventional controller pairings and settings

Control loop	Controller gain	Integral time (min)	Remark
y_1, u_4	0.0013	70.0	Gain scheduling
y_2, u_1	0.04	30.0	
y_3, u_2	0.2	60.0	Gain and integral time scheduling
y_4, u_6	0.2	120.0	Bias term
y_5, u_5	0.01	120.0	

However, a more modern approach in the form of a multivariable controller is preferred, since it takes care of all the process interactions.

7. Conclusions

For two heat integrated distillation towers a first principles dynamic model was developed which provided good prediction capabilities.

All concentration responses and the pressure response showed a minor influence of the vapor hold-up, which is in contradiction with the literature, where it is suggested to include the vapor hold-up in the model for high pressure, low temperature columns. It was found that this depends strongly on the capacity for pressure changes and the resistance to flow changes.

From the detailed, validated model, step weight models were derived at minimum and maximum process conditions and it was investigated whether a multivariable model predictive controller with fixed settings could be used to control the process. A stable multivariable controller could be designed for the entire operating region, provided the range of the manipulated variables would be sufficient.

Controller performance for set-point changes is good, provided changes in process inputs are constrained in order to avoid temporary saturation of inputs. Controller disturbance rejection for the most common disturbance was good for step changes up to 10%, and from a comparison with operating experience with conventional PI control with gain scheduling, feed-forward and decoupling, it was found that multivariable control provided an improvement. Also valve saturation could be avoided in case of multivariable control by proper controller tuning whereas this proved to be very difficult to almost impossible in case of single loop controllers.

Nomenclature

A	area (m^2)
β	aeration factor
c	specific heat (kJ^{-1} kg^{-1} K^{-1})
c_1	constant in heat transfer equation
C	capacity for pressure/flow changes (kmol bar^{-1})
d_i	disturbance variable, $i = 1, \ldots, 3$ (kmol min^{-1})

E	energy (kJ)
eff	tray efficiency
ϕ	relative froth density
F	flow (kmol s^{-1})
g	acceleration of gravity (m s^{-2})
h	enthalpy (kJ $kmol^{-1}$) or liquid height (m)
K	vapor–liquid equilibrium constant
l	length (m)
M	total mass or hold-up (kmol)
Mc	mass individual component (kmol)
mw	molecular weight (kg $kmol^{-1}$)
p	pressure (bar)
Δp	pressure drop (bar)
Q	energy transferred in reboiler–condenser (kW)
R	restistance for flow changes (bar s $kmol^{-1}$)
T	temperature (K)
U	overall heat transfer coefficient (kJ K^{-1} s^{-1} m^{-2})
u_i	manipulated process variable, $i = 1, \ldots, 6$ (kmol min^{-1})
V	volume (m^3)
$\bar{V}$	average column volume (m^3)
x	liquid mole fraction
y_i	vapor mole fraction, i = letter
y_i	controlled process variable, $i = 1, \ldots, 5$

Subscripts

c	component identifier
cross	cross section of tray
f	froth
GO2	gaseous oxygen
L	liquid
Lin	liquid entering tray
Lout	liquid leaving tray
nocomp	number of components
ow	over weir
ref	reference
V	vapor
Vin	vapor entering tray
Vout	vapor leaving tray
t	tray
ρ	density (kg m^{-3})

Appendix A

Laws of conservation

The total mass of component c on a tray is given by:

$$Mc_c = M_V y_{Vout,c} + M_l x_{Lout,c} \quad \forall\, c \in \{1 \ldots \text{nocomp}\} \tag{A1}$$

The component balance for a tray is:

$$\frac{dMc_c}{dt} = F_{Vin} y_{Vin,c} + F_{Lin} x_{Lin,c} - F_{Vout,c} y_{Vout,c} - F_{Lout} x_{Lout,c} \quad \forall\, c \in \{1 \ldots \text{nocomp}\} \tag{A2}$$

The total mass on a tray can be calculated from the sum of the mass of the individual components:

$$M = \sum_{c=1}^{\text{nocomp}} Mc_c \tag{A3}$$

The energy contents of the tray can be given by:

$$E = M_V h_{Vout} + M_l h_{Lout} + M_t c_t (T_{Lout} - T_{ref}) \tag{A4}$$

and the energy balance for a tray is:

$$\frac{dE}{dt} = F_{Vin} h_{Vin} F_{Lin} h_{Lin} - F_{Vout} h_{Vout} - F_{Lout} h_{Lout} \tag{A5}$$

Tray hydraulics

Aeration of the liquid on the tray can be calculated using an aeration factor β (Gallun & Holland, 1982)

$$\beta = 1 - 0.3593 \left(\frac{F_{Vin} mw_v}{A_{cross} \sqrt{\rho_v}} \right)^{0.177709} \tag{A6}$$

Hutchinson (1949) showed that the relative froth density ϕ depends on the aeration factor β according to:

$$\phi = 2\beta - 1 \tag{A7}$$

The amount of liquid leaving the tray can be determined using the law of Bernoulli which leads to the well-known Francis equation. Taking the relative froth density into account it becomes:

$$F_{Lout} = \frac{2}{3} \sqrt{2g} \frac{\rho_l}{mw_l} l_{weir} \phi h_{ow}^{3/2} \tag{A8}$$

In this equation h_{ow} is the weir height:

$$h_{ow} = h_f - h_w \tag{A9}$$

The froth height h_f is given by:

$$h_f = \frac{M_l mw_l}{A_{cross} \rho_l \phi} \tag{A10}$$

The dry tray pressure drop can be calculated, amongst others, from the equation (Gani, Ruiz & Cameron, 1986):

$$\Delta p_{dry} = 0.0013 \left(\frac{F_{Vin} mw_v}{A_{holes} \rho_v} \right)^{1.08} \tag{A11}$$

The required pressure drop to sustain the vapor flow can be calculated from the total pressure drop minus the pressure drop due to the liquid height on the tray:

$$\Delta p_{tot} = p_{Vin} - p_{Vout} = \Delta p_{dry} + \beta \frac{M_l mw_l}{A_{cross}} g * 10^5 \tag{A12}$$

Equilibrium equations

Based on the assumption that the liquid, which is in contact with the vapor, is in equilibrium, the vapor concentration can be computed from:

$$y_c = K_c x_c \quad \forall c \in \{1 \ldots \text{nocomp}\} \tag{A13}$$

However, the tray efficiency (eff) need not always be 100%, hence the effective concentration of the vapor leaving the tray becomes (see Fig. 3):

$$y_{\text{Vout,c}} = \text{eff} K x_{\text{Lout,c}} + (1 - \text{eff}) y_{\text{Vin,c}} \quad \forall\, c \in \{1 \ldots \text{nocomp}\} \tag{A14}$$

The value of K depends on the components present in the mixture and follows from the physical properties data bank.

Physical properties

The physical properties of a mixture of components are a function of pressure, temperature and composition. They are calculated using the Peng-Robinson equation of state. The molar volume is determined using the API method or the relationship of Rackett (Speedup Manual, 1992).The following proprietary properties are used:

$$h_{\text{Vout}} = \text{enth\_mol\_vap}(T_{\text{Vout}}, p_{\text{Vout}}, y_{\text{Vout}}) \tag{A15}$$

$$h_{\text{Lout}} = \text{enth\_mol\_liq}(T_{\text{Lout}}, p_{\text{Lout}}, x_{\text{Lout}}) \tag{A16}$$

$$K_c = \text{kvalues}(T_{\text{Vout}}, p_{\text{Vout}}, x_{\text{Lout}}, y_{\text{Vout}}) \tag{A17}$$

Additional equations

There are a number of additional equations, which are required to complete the model description. The temperature and pressure on a tray are uniform, i.e. $p_{\text{Lout}} = p_{\text{Vout}}$ and $T_{\text{Lout}} = T_{\text{Vout}}$. The sum of the fractions in the liquid and vapor phase are equal to one.

$$\rho_v = \text{dens\_mass\_vap}(T_{\text{Vout}}, p_{\text{Vout}}, y_{\text{Vout}}) \tag{A18}$$

$$mw_v = \text{molweight}(y_{\text{Vout}}) \tag{A19}$$

$$mw_l = \text{molweight}(x_{\text{Lout}}) \tag{A20}$$

$$\rho_l = \text{dens\_mass\_liq}(T_{\text{Lout}}, p_{\text{Lout}}, x_{\text{Lout}}) \tag{A21}$$

The sum of the volume of the liquid and vapor must equal the tray volume:

$$V_t = \frac{M_l mw_l}{\rho_l} + \frac{M_v mw_v}{\rho_v} \tag{A22}$$

There are a number of trays, on which feed is entering or from which product is withdrawn. In principle the described set of tray equations can be used; they have to be modified to include the additional flow with associated properties.

References

Skogestad, S., *Dynamics and control of distillation columns-a critical survey*, 3rd IFAC Symposium DYCORD + , College Park, MA, 1992.

Mandler, J. A., Vinson, D. R., & Chatterjee, N. (1989). 2nd IFAC Symposium DYCORD + , Maastricht, August, 1989, pp. 267–273.

Gross, F., Baumann, E., Geser, E., Rippin, D. W. T., & Lang, L. (1998). Modelling, simulation and controllability analysis of an industrial heat-integrated distillation process. *Computers & Chemical Engineering*, *22*(1–2), 223–237.

Gallun, S., & Holland, C. D. (1982). *Computers and Chemical Engineering*, *6*(3), 231–244.

Hutchinson, M. H. (1949). *Aerated flow principles applied to sieve plates*, Paper presented at the AIChE Meeting, Los Angelos, CA, May, 1949.

Gani, R., Ruiz, C. A., & Cameron, I. T. (1986). *Computers & Chemical Engineering*, *10*(3), 181–198.

Rademaker, O., Rijnsdorp, J. E., & Maarleveld, A. (1975). *Dynamics and control of continuous distillation units*. Amsterdam: Elsevier.

Luyben, W. L. (1992). *Practical distillation control* (p. 1992). New York: Van Nostrand Reinhold.

Speedup Manual, Aspen Tech. Inc., 1992